High speed optical transmission utilizing constant envelope modulation based on frequency shift keying and minimum-shift keying

(Invited Paper)

Nan Chi (迟 楠)*, Wuliang Fang (方武良), Yufeng Shao (邵宇丰), Junwen Zhang (张俊文), Bo Huang (黄 博), Jiangbo Zhu (朱江波), and Li Tao (陶 理)

Department of Communication Science and Engineering, State Key Lab of ASIC and System, Fudan University, Shanghai 200433, China

**E-mail: nanchi@fudan.edu.cn*

Received June 17, 2010

A novel 40-Gb/s constant envelope optical frequency shift keying (FSK) transmitter and the transmission characteristics are investigated both by simulation and experiment. Meanwhile, to increase the spectrum efficiency of FSK, we propose a novel optical minimum-shift keying (MSK) scheme and analyze its performance compared with other MSK schemes and other traditional modulation formats. Simulation and experimental results show that the novel FSK scheme could be a potential candidate for the future high speed transmission and label switching systems. And the novel MSK scheme deserves future deep research for its potential excellent performance.

OCIS codes: 060.2330, 060.2360, 060.4080.
doi: 10.3788/COL20100809.0837.

Recently, with the development of optical devices, large quantities of advanced modulation formats, such as differential quadrature phase shift keying (DQPSK), quadrature amplitude modulation (QAM), and so on, which have just been widely used in electrical communication systems, have attracted increased attention in the field of optical communication, in order to enhance optical signal's robustness to chromatic dispersion and fiber nonlinear effects, or require less bandwidth of electrical circuits[1−10]. Of the advanced modulation formats, constant envelop modulation formats such as differential phase shift keying (DPSK), frequency shift keying (FSK), and so on are focused on for their outstanding nonlinearity resilience[6−9]. As a particular constant envelope modulation format, FSK enables differential detection scheme and simulations have shown that it has comparable gain of optical signal-to-noise ratio (OSNR) sensitivity to DPSK in 10-Gb/s transmission systems[8]. It can also be used for payload or label modulation in the orthogonal optical labeling schemes as it is orthogonal to the conventional on-off keying (OOK) modulation format[11−13]. Therefore, FSK could be one of the most potential solutions for future high-speed transmission systems and optical packet switching networks[14−20].

FSK signal can be generated by direct modulation of electric current in a laser light source, e.g., a distributed feedback (DFB) laser[15] or a grating-assisted co-directional coupler with sampled grating reflector (GCSR) laser[13]. This idea, however, is limited by the relatively low frequency modulation response of the laser and has a detrimental effect of parasitic intensity modulation. In order to generate a high speed FSK signal at 40 Gb/s and above, a scheme was reported to utilize a specially designed $LiNbO_3$ external FSK modulator[17]. However, this scheme requires relatively complicated manufacturing and integration. We have reported another scheme based on phase modulation and phase-to-amplitude conversion[20].

Although FSK modulation is outstanding in performance, its relatively low spectrum efficiency is a fatal disadvantage. So optical minimum-shift keying (O-MSK) is introduced. As a special kind of FSK modulation, minimum-shift keying (MSK) modulation is well known in wireless communication area for its high spectrum efficiency and continual phase shifting. Recently, some researchers have introduced MSK in optical communication system to fight against dispersion and nonlinearity[21−23].

In this letter, a novel 40-Gb/s FSK transmitter and the transmission characteristics are investigated both by simulation and experiment. Meanwhile, we propose a novel O-MSK scheme and analyze its performance compared with other MSK schemes and other traditional modulation formats.

The schematics of the FSK as well as return-to-zero (RZ) FSK generation and detection are illustrated in Figs. 1(a) and (b). To generate a FSK signal as high as 40 Gb/s and above, two continuous-wave (CW) lasers are combined by a 3-dB coupler and then input to a Mach-Zehnder modulator (MZM1) or a phase modulator (PM), which is modulated by non-return-zero (NRZ) data, and are then demodulated to intensity modulation by the subsequent Mach-Zehnder delay interferometer (MZDI). The MZDI is imbalanced by introducing one-bit time delay line. The wavelengths of the two CW beams are carefully selected so that one is at the maximum transmission of the MZDI (constructive interference) while the other at the minimum (destructive interference). Thus the tone spacing is $(N + 1/2)/T_b$ Hz (N=1, 2, 3,$\cdots$), where T_b is one bit period. Assuming that the center frequencies

of the two beams are f_1 and f_2, respectively, the optical fields exiting a phase modulator are given by

$$E_1(t) = E_0 \cdot \exp\left(\mathrm{j}\frac{2\pi f_1 T_\mathrm{b} + \Phi_1 + \Phi_2}{2}\right) \cdot \cos\left(\frac{2\pi f_1 T_\mathrm{b} + \varphi}{2}\right), \quad (1)$$

$$E_2(t) = E_0 \cdot \exp\left(\mathrm{j}\frac{2\pi f_2 T_\mathrm{b} + \Phi_1 + \Phi_2}{2}\right) \cdot \cos\left(\frac{2\pi f_2 T_\mathrm{b} + \varphi}{2}\right), \quad (2)$$

where Φ_1, Φ_2 are the phases of the neighboring bits, and the data information is reflected in the phase difference φ. Using the fact that

$$f_1 = \frac{m}{T_\mathrm{b}} \quad (m = 0, 1, 2, \cdots, M), \quad (3)$$

and

$$f_2 = f_1 + \frac{2n+1}{2T_\mathrm{b}} \quad (n = 0, 1, 2, \cdots, N), \quad (4)$$

the frequency tone spacing (FTS) of the generated FSK signal should be expressed as

$$\mathrm{FTS} = \frac{2n+1}{2T_\mathrm{b}} \quad (n = 0, 1, 2, \cdots, N). \quad (5)$$

While the coupling ratios of the MZDI's two couplers are both 50:50, the output at the constructive port of MZDI can be described by

$$P_\mathrm{o} = P_\mathrm{i} \cdot \left\{ -\frac{1}{2}\cos\left[(2\pi f_1 + 2\pi f_2)\cdot \mathrm{FTS} + \Delta\varphi + \frac{\pi}{2}\right] + \frac{1}{2}\right\}, \quad (6)$$

where P_i and P_o are the input and output optical power, $\Delta\varphi$ is the phase difference between the two arms of MZDI. According to Eq. (6), if the central frequency of the laser is located at such a position that one of the generated FSK tones (f_1) is located exactly at the maximum transmission point of the MZDI while the other (f_2) at the minimum transmission point, as depicted in Fig. 1(c), two logically inverted data streams can be achieved at each MZDI output. In this way, an optical FSK signal is generated at the output of MZDI. The FSK signal with an optical pulse existing at every bit slot is generated. It should be noted that the constructive wavelength carries duobinary (DB) modulation, whereas the destructive one carries alternate-mark inversion (AMI)[2]. Hence, the FSK signal can be regarded as the combination of two intensity-modulated (IM) signals with non-information-bearing phase modulation.

In practice, the frequency modulation format with RZ shape is widely used in long-haul optical communication systems due to its superior performance. The RZ pulse carver can be implemented cascading another MZM (MZM2) after MZDI. In our scheme, the MZM2 driven by a sinusoidal voltage at half of the bit rate is employed. As a result, the generated FSK signal passes through MZM2 to generate a RZ-FSK signal. Figure 1(b) shows the configuration of the RZ-FSK receiver. The optical band-pass filter (OBPF) provides more than 25 dB suppression ratio between the two FSK tones. An array waveguide grating (AWG) demultiplexer is used to separate the two FSK tones and demodulate the FSK into intensity modulation. As discussed before, the data stream obtained at one output is identical to the original one, but at another output, the detected data stream is logically inverted. Hence these two outputs can be detected by a differential receiver. A low pass filter is applied after the differential

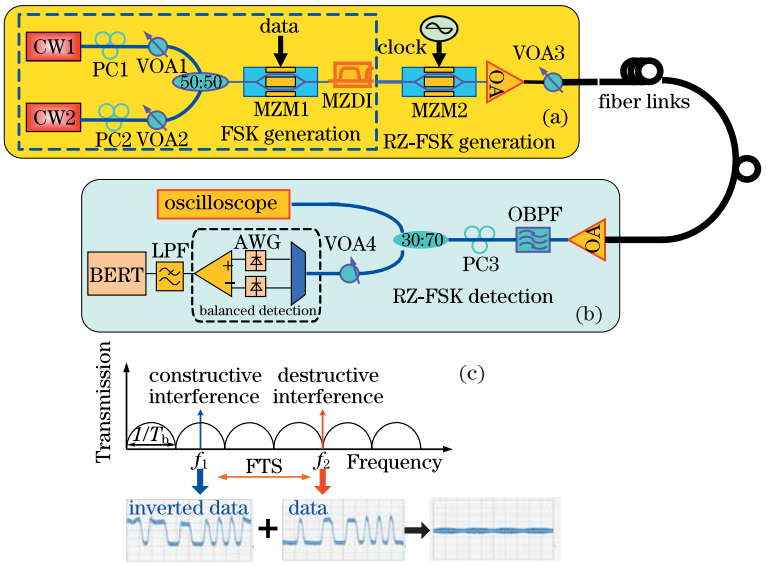

Fig. 1. Principle of RZ-FSK generation and detection and the generated FSK signal by experiment. (a) Configuration of our proposed transmitter. (b) Configuration of the used receiver. (c) Generation of FSK signal. PC: polarization controller; VOA: variable optical attenuator; OA: optical amplifier; OBPF: optical band-pass filter; OSC: oscilloscope; AWG: array waveguide grating; PD: photodiode; LPF: low pass filter; BERT: bit error rate tester.

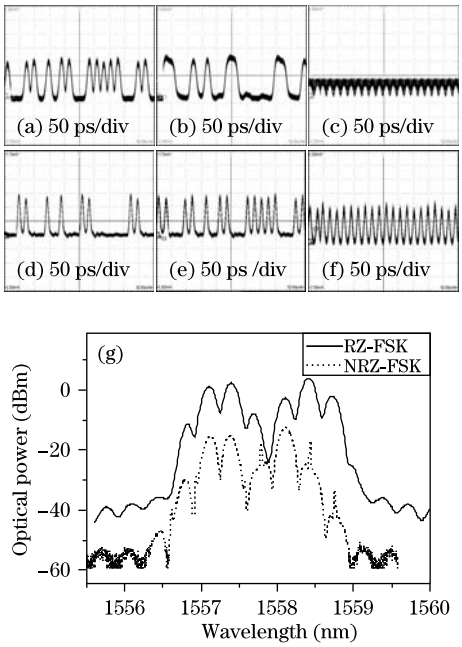

Fig. 2. Waveforms measured by experiment for (a) NRZ-FSK tone 1, (b) NRZ-FSK tone 2, (c) NRZ-FSK, (d) RZ-FSK tone 1, (e) RZ-FSK tone 2, (f) RZ-FSK, and (g) optical spectra curves for NRZ-FSK signal and RZ-FSK signal.

electrical amplifier to remove the high-frequency pulses induced by the beating of the two modes. Figure 2 shows the measured waveforms and optical spectra for FSK and RZ-FSK signals. Clear waveforms powerfully demonstrate the feasibility of the proposed FSK and RZ-FSK generation schemes. From Fig. 2(g) with conventional spectra, two non-symmetrical FSK components and RZ-FSK components can be observed, which are generated with the proposed scheme. It can be well explained by the fact that the FSK signal is obtained by demodulating two DPSK signals. According to the positions of the two RZ-FSK tones shown in Fig. 2(g), the low-frequency RZ-FSK component carries the spectrum of RZ-DB modulation format and the high-frequency one represents the spectrum of RZ-AMI modulation format. The degree of overlapping of these two spectral components will be increased with the decrease of tone spacing.

MSK is a special kind of FSK modulation format, for which the FTS is $1/2T_{\rm b}$, the minimum value among all FSK schemes. What's more, the phase of optical signal is just continually changing, which makes its sidebands decay fast and hence it is considered to be a very promising high speed modulation technology.

Because of its special characteristics, MSK cannot be produced by traditional FSK methods. We propose a novel MSK scheme, of which the system configuration is shown in Fig. 3. It is mainly formed by 4 same MZMs. The continual laser source is divided into two beams that are modulated by MZM1 and MZM3 separately. As MZM1 and MZM3 are differently biased (MZM1 is biased at $V_{\pi/2}$, while MZM3 is biased at V_{π}), two carrier suppressed RZ (CSRZ) signals with different duty cycles are produced. Then they are coupled into MZM2 and MZM4 respectively, driven by the two-way signals which are formed by splitting the pre-coded high speed bit stream into the even and odd parts. Finally, the modulated CSRZ signals are combined together to get optical MSK signals. The comparison of spectrum between MSK and BPSK with the same modulation bitrate is shown in Fig. 4. As well known, in MSK transmitter, it is critical to produce standard sinusoidal shape carrier. It has been demonstrated that for such a kind of nonlinear modulator as MZM, a triangle drive signal should be used to get sinusoidal shape optical signals from the output of modulators. Unfortunately, in the situation where the bit rate is as high as 40 Gb/s, it is really hard and costly to produce triangle drive signal. In our scheme, we just utilize sinusoidal signal to drive MZM and accurately manage the bias points of all MZMs as well as the pre-coding process, and successfully realize high quality MSK modulation.

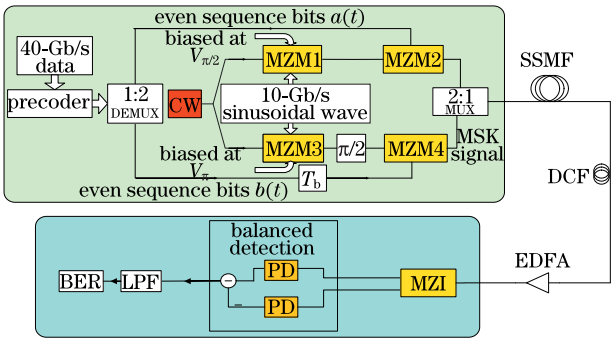

Fig. 3. Novel scheme of MSK transceiver. DEMUX: demultiplexer; MUX: multiplexer; MZI: Mach-Zehnder interferometer.

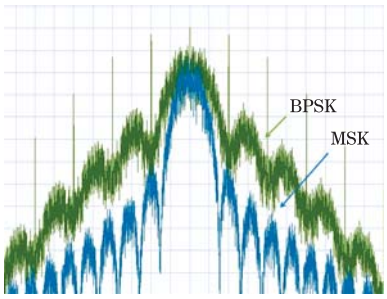

Fig. 4. Comparison of spectrum between MSK and BPSK with the same modulation bit rate.

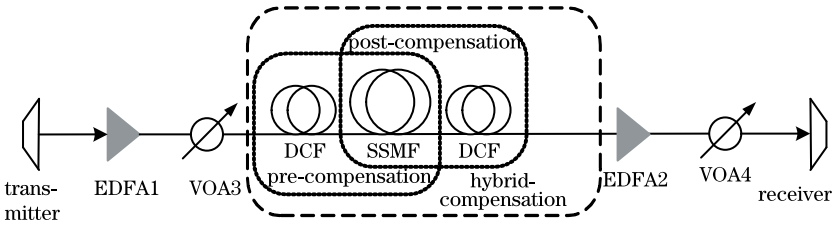

Fig. 5. Transmission link with three different schemes to compensate the fiber dispersion.

Table 1. Used Optical Fiber Parameters

Fiber	SMF	DCF
Dispersion D (ps/(nm·km))	16	– 90
Fiber Loss (dB/km)	0.2	0.6
Nonlinear Coefficient γ $((\mathrm{W\cdot km})^{-1})$	2.6	4
Dispersion Slope $\mathrm{d}D/\mathrm{d}\lambda$ $(\mathrm{ps/(nm^2\cdot km)})$	0.08	– 0.21

The simulation configuration is shown in Fig. 5. An erbium-doped fiber amplifier (EDFA) is set at the beginning of each span to compensate signal attenuation in the signle-mode fiber (SMF) and its matching disperision compensating fiber (DCF), followed by a variable optical attenuator (VOA) to adjust the span launch power. The transmission fiber parameters are shown in Table 1.

The system performances with different dispersion compensation schemes are studied for FSK, DPSK, and RZ respectively by simulation. As for FSK, it is found that 1-dB tolerance range of the compensation ratio between 98% and 102% corresponds to a residual dispersion of 26 ps/nm, which is almost half of the dispersion tolerance of RZ and DPSK. In this simulation, the DPSK signal is produced by a phase modulator and the RZ signal is generated by push-pull RZ modulation followed by the NRZ modulation. Due to the relatively large signal bandwidth, the dispersion should be carefully managed for the transmission of FSK signal.

Figure 6 shows the simulation results on how the dispersion compensation scheme and the span input power affect the system performance over 11 spans of 80-km transmission link. Multi-span transmission over 880-km SMF is achieved for FSK. When the receiver sensitivity is defined as the received optical power at bit error rate (BER) of 10^{-9}, given the same sensitivity penalty, DPSK has the maximum reach whereas RZ the minimum. For FSK and DPSK, post-compensation scheme has better performance than pre-compensation, while for RZ, pre-compensation is preferred. The tolerance to nonlinear effects is demonstrated in Fig. 6 where the sensitivity penalty is calculated from each span input power. At low powers, the performance is degraded by the amplified spontaneous emission (ASE) noise from the amplifiers. If the power is increased, self-phase modulation in conjunction with dispersion will degrade the signal. Between two extremes the optimized range of input power is around 5–8 dBm for FSK. It is clear that the generated FSK signal shows high fiber input power tolerance for long distance transmission link with post-compensation.

Figures 7 and 8 show the transmission performances of FSK and RZ-FSK formats. It is demonstrated that the transmission performance of the RZ-FSK format is better under all the three dispersion compensation schemes.

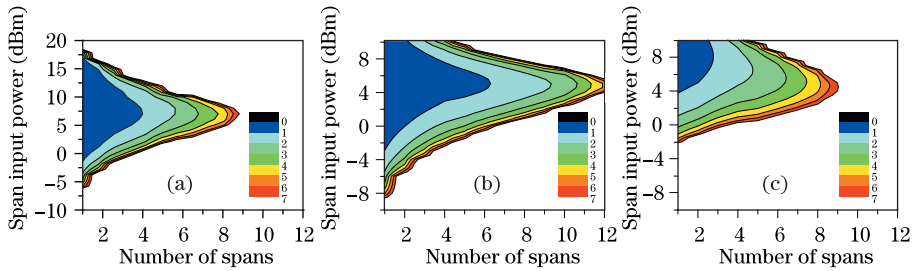

Fig. 6. Receiver sensitivity penalty as a function of the span input power and the number of spans for (a) FSK with post-compensation scheme, (b) DPSK with post-compensation scheme, and (c) 33% RZ with pre-compensation scheme.

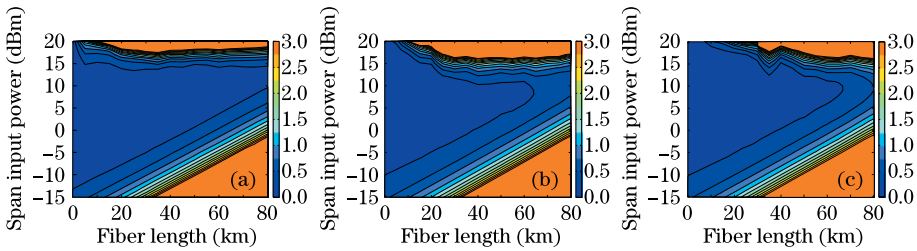

Fig. 7. Contour plots of receiver sensitivity for the FSK signal as a function of input power and fiber length for (a) post-compensation, (b) pre-compensation, and (c) hybrid-compensation.

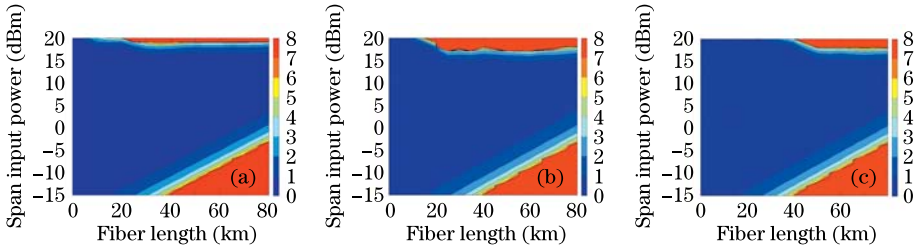

Fig. 8. Contour plots of receiver sensitivity for the RZ-FSK signal as a function of input power and fiber length for (a) post-compensation, (b) pre-compensation, and (c) hybrid-compensation.

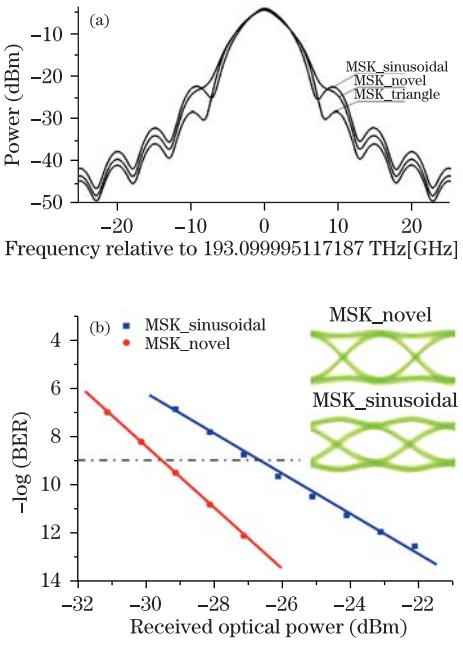

Fig. 9. Comparison of (a) optical spectrum and (b) BER performance among different MSK schemes.

Firstly, the receiver power penalty of the RZ-FSK format is lower than that of the FSK format. Secondly, the resilience of input power level is considerable for the RZ-FSK format. Finally, the RZ-FSK modulation format also has better dispersion tolerance. With the comparison between FSK and RZ-FSK formats, we can find the optimum frequency modulation format for high bit rate optical transmission systems. Our novel scheme of MSK is proposed to promote the spectrum efficiency of FSK. As shown in Fig. 4, the spectrum characteristic of MSK is quite excellent. Now we consider the BER performance of our MSK scheme compared with the existing MSK schemes and other modulation formats. The reported MSK schemes are mainly two kinds[21−23], one is the triangle driven scheme and the other is sinusoidal driven method. The comparison between the existing schemes and our scheme are shown in Fig. 9. It can be found that the spectrum of our scheme is just close to triangle scheme while better than traditional sinusoidal scheme. Simulation results show that when the MZM is driven by standard triangle signal, it would output perfect sinusoidal shape optical signals. The shortcoming of such a scheme is the unavailability of triangle signal at high bitrate. Our scheme is aimed to improve the performance of an alternative for triangle scheme — sinusoidal driven scheme. The BER performance comparison between our scheme and traditional sinusoidal scheme is shown in Fig. 9(b), which illustrates that the receiver sensibility of our scheme at a BER of 10^{-9} is about 3 dB better than the sinusoidal one. Although in our scheme, the continuity of phase is not quite good, the optical signal power keeps constant, which just explains why the power penalty with residual dispersion of our scheme is lower than that of the sinusoidal scheme. Under present device condition, with a tradeoff between availability and quality, our novel MSK scheme is a quite promising alternative for high speed transmission system.

The experimental setup is shown in Fig. 10. The signal sources include an external cavity laser (ECL) at 1557.64 nm and a tunable laser made by Agility Inc. at 1558.46 nm, i.e., with 100-GHz FTS. In this experiment, we launch RZ-FSK signal with 100-GHz FTS, since it has been proved that such a signal is more suitable for its lower power penalties and relatively easier design of receiver compared with RZ-FSK signal with 60-GHz FTS. It is noted that two beams can be generated by a MZM driven by 50-GHz clock. The data at 40-Gb/s (pseudo-random bit sequence (PRBS) 2^{23}–1, ITU-T G.709 FEC) is generated by SHF BPG44E BT pattern generator and added onto the MZM1. The phase-modulated signal is then demodulated by the subsequent MZDI with 25-ps delay, thus realizing a 40-Gb/s FSK signal. A following MZM2 is driven by 20-GHz clock and used to generate RZ-FSK signal. It should be noted that the output power of two lasers has to be fine tuned so that an approximately constant optical pulse would be achieved by the RZ-FSK transmitter. The transmission span consists of 100-km-long SMF with a matching length of DCF for post-compensation. We choose post-compensation in the experimental scheme, because the above simulations prove that the post-compensation has good receiver performance and it is easily implemented in practice. The dispersions at 1550 nm of the SMF and DCF are 16.9 and –100 ps/(nm·km), respectively. In each span, the SMF input power is 6 dBm, and the DCF input power is 0 dBm.

At the receiver, the frequency discrimination for RZ-FSK demodulation is achieved by an OBPF2 with

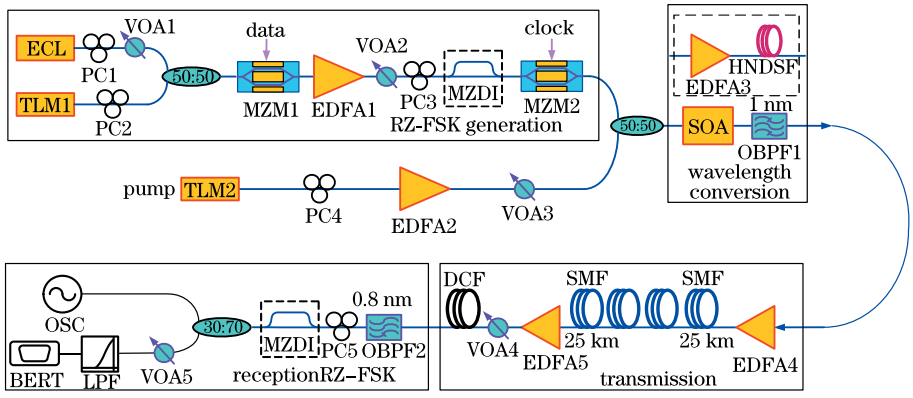

Fig. 10. Experimental setup. ECL: external cavity laser; TLM: tunable laser modulator; HNDSF: highly nonlinear dispersion shifted fiber; SOA: semiconductor optical amplifier.

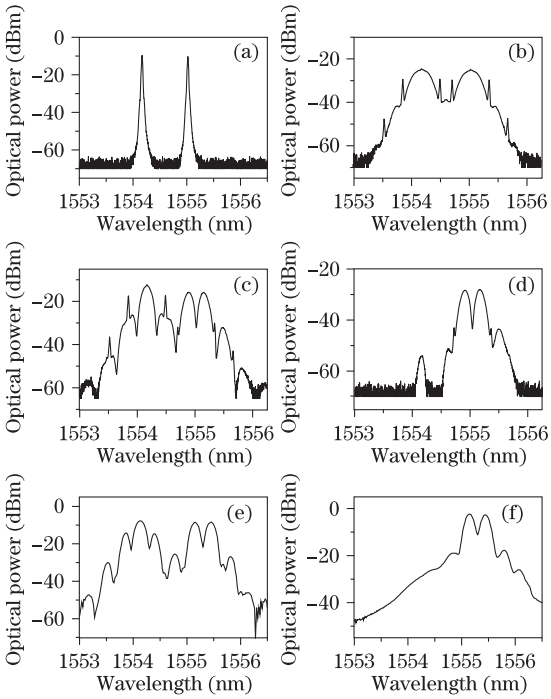

Fig. 11. Measured optical spectra for (a) CW light signal, (b) after DPSK modulation, (c) FSK signal, (d) demodulated FSK signal, (e) RZ-FSK signal, (f) demodulated RZ-FSK signal.

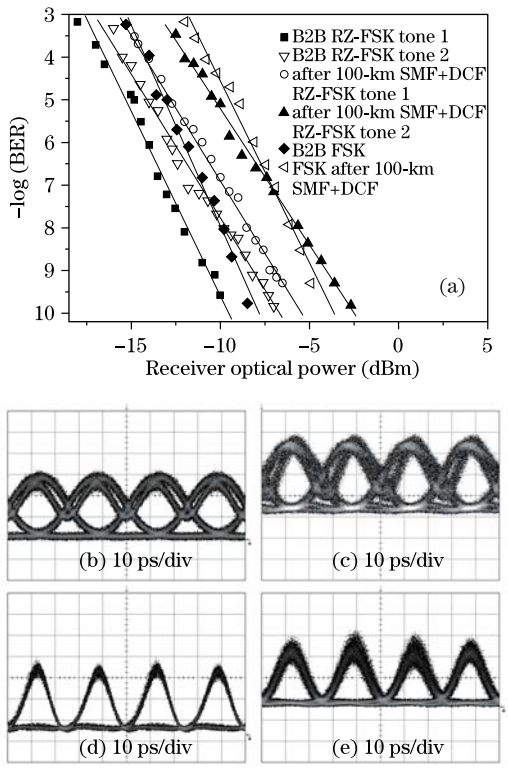

Fig. 12. Measured BER curves for (a) back-to-back (B2B) RZ-FSK and after 100-km SMF+DCF link, the eye diagrams of demodulated FSK for (b) B2B and (c) after 100-km SMF+DCF link, and the eye diagram of demodulated RZ-FSK for (d) B2B and (e) after 100-km SMF+DCF link.

0.8-nm bandwidth filter which provides more than 25 dB suppression ratio between the two FSK tones. This demodulated signal is detected by SHF 47100A V/E converter and the BER is measured by SHF EA44 error analyzer.

Figure 11 shows the measured optical spectra of CW light signal, signal after DPSK modulation, FSK signal, demodulated FSK signal, RZ-FSK signal, and demodulated RZ-FSK signal. We can find that an improved transmission characteristic for the RZ-FSK signal can be achieved compared with the FSK signal. The measured BER curves before and after the transmission link are shown in Fig. 12(a), where error-free transmissions for RZ-FSK and FSK can be obtained. The power penalty against the FSK at the BER of 10^{-9} is about 5.0 dB. The transmission penalties for tone1 and tone2 of RZ-FSK are both less than 5 dB. Figures 12(b)–(e) show back-to-back eye-diagrams of FSK and RZ-FSK, and eye-diagrams after transmission through a 100-km SMF transmission link with matching DCF. Because FSK is orthogonal to intensity modulation and vector modulation (polarization shift keying), it can be employed in the context of the combined modulation format to decrease the data rate or enhance the symbol rate. It can also be utilized in orthogonal labeling as the modulation format for the payload or the label.

In conclusion, a novel 40-Gb/s optical FSK transmitter and the transmission characteristics are investigated. To increase the spectrum efficiency of FSK, we propose a novel O-MSK scheme and analyze its performance compared with other MSK schemes and other traditional modulation formats. Simulation and experimental results show that the novel FSK scheme could be a potential candidate for the future high speed transmission and label switching systems. And the novel MSK scheme deserves future deep research for its potential excellent performance.

This work was partially supported by the National "973" Program of China (No. 2010CB328300), the National Natural Science Foundation of China (Nos. 600837004 and 60777010), the National "863" Program of China (Nos. 2009AA01Z253, 2009AA01A347, and 2007AA01Z260), the Chinese Postdoctoral Science Foundation (No. 20090460593), Shanghai Postdoctoral Science Foundation (No. 10R21411600), the Open Fund of Beijing University of Posts and Telecommunications, and the Shuguang Fund.

References

1. P. J. Winzer and R. J. Essiambre, in *Proceedings of ECOC 2003* Th2.6.1 (2003).
2. A. Gnauck and P. Winzer, J. Lightwave Technol. **23,** 115 (2005).
3. Y. Han and G. F. Li, IEEE J. Sel. Top. Quantum Electron. **12,** 571 (2006).
4. Y. Shao, S. Wen, L. Chen, Y. Li, and H. Xu, Opt. Express **16,** 12937 (2008).
5. Y. Shao, S. Wen, L. Chen, and J. Yu, Chinese J. Lasers (in Chinese) **35,** 1201 (2008).
6. Y. Shao, J. Li, L. Cheng, Y. Pi, S. Wen, and L. Chen, Chinese J. Lasers (in Chinese) **35,** 574 (2008).
7. Y. Shao, L. Chen, S. Wen, Y. Xiao, L. Cheng, H. Xu, and Y. Pi, Opt. Commun. **281,** 3658 (2008).
8. W. Idler, A. Klekamp, R. Dischler, and B. Wedding, in *Proceedings of 2004 IEEE/LEOS Workshop on Advanced*

Modulation Formats FD3 (2004).

9. J. Zhang, Y. Shao, W. Fang, B. Huang, D. Huang, and N. Chi, Acta Opt. Sin. (in Chinese) **30,** 1971 (2010).
10. Y. Shao, L. Chen, and S. Wen, Microw. Opt. Technol. Lett. **49,** 755 (2007).
11. J. Zhang, N. Chi, P. V. Holm-Nielsen, C. Peucheret, and P. Jeppesen, IEEE Photon. Technol. Lett. **15,** 1174 (2003).
12. T. Kawanishi, K. Higuma, T. Fujita, J. Ichikawa, T. Sakamoto, S. Shinada, and M. Izutsu, J. Lightwave Technol. **23,** 87 (2005).
13. Y. Yu, G. Mulvihill, S. O'Duill, and R. O'Dowd, IEEE Photon. Technol. Lett. **16,** 39 (2004).
14. E. N. Lallas, N. Skarmoutsos, and D. Syvridis, J. Lightwave Technol. **23,** 1199 (2005).
15. N. Chi, J. Zhang, P. V. Holm-Nielsen, L. Xu, I. T. Monroy, C. Peucheret, K. Yvind, L. J. Christiansen, and P. Jeppesen, Electron. Lett. **39,** 676 (2003).
16. E. N. Lallas, N. Skarmoutsos, and D. Syvridis, J. Lightwave Technol. **23,** 1199 (2005).
17. T. Kawanishi, T. Sakamoto, T. Miyazaki, and M. Izutsu, Opt. Express **14,** 4469 (2006).
18. A. Hodžić, B. Konrad, and K. Petermann, J. Lightwave Technol. **20,** 598 (2002).
19. Y. Shao, N. Chi, C. Hou, W. Fang, J. Zhang, B. Huang, X. Li, S. Zou, X. Liu, X. Zhang, N. Zhang, Y. Fang, J. Zhu, L. Tao, and D. Huang, J. Lightwave Technol. **28,** 1770 (2010).
20. N. Chi and S. Yu, in *Proc. ECOC'05* We4.P.114 (2005).
21. J. Mo, Y. J. Wen, Y. Wang, C. Lu, and W.-D. Zhong, J. Lightwave Technol. **25,** 3151 (2007).
22. M. Ohm and J. Speidel, in *Proc. APOC 2003* 5281-23 (2003).
23. K. Higuma and J. Ichikawa, in *Proc. ECOC 2009* Th3.D.5 (2009).